Quantization of Widefield Fluorescence Images Using Structured Illumination and Image Analysis Software

ANDREW L. BARLOW[1*] AND CHRISTOPHER J. GUERIN[2]
[1]*Improvision Ltd., Viscount Centre II, University of Warwick Science Park, Millburn Hill Road, Coventry, United Kingdom*
[2]*Medical Research Council, Toxicology Unit, Hodgkin Building, Lancaster Road, Leicester, United Kingdom*

KEY WORDS quantitative studies; measurements; transferrin; internalization; intensity

ABSTRACT It is difficult to obtain precise quantitative measurements from fluorescent images captured from widefield microscopes. We wished to ascertain if reliable quantitative measurements of both biological and nonbiological specimens were possible using a widefield microscope equipped with a structured illumination system and image analysis software. In a nonbiological specimen, images were obtained from fluorescent beads of known intensity. For a biologically relevant model we used the uptake of fluorescently labeled transferrin by HeLa cells in culture. In the bead sample, the mean intensity of beads acquired with the structured illumination system showed relative intensities near to the predicted values without any further manipulation of data. In the transferrin uptake experiments, uptake and subsequent recycling of the labeled transferrin could be accurately and reproducibly measured. We conclude that using a combination of structured illumination and image processing algorithms accurate quantization of fluorescent images can be achieved in widefield microscopy *Microsc. Res. Tech. 70:76–84, 2007.*

INTRODUCTION

Quantitative fluorescence microscopy can be a valuable tool to dissect the details of biological processes but can be difficult to achieve because of artifacts arising in image acquisition using widefield microscopes. Such artifacts arise from the fact that widefield microscopes illuminate the whole of the sample simultaneously and are incapable of eliminating light that originates in focal planes other than the plane being imaged (Conchello and Lichtman, 2005; Yuste, 2005). This greatly degrades the quality of 3D volumes acquired with widefield microscopes and greatly complicates any quantization attempted.

Recently, structured light illumination systems have been introduced to overcome this limitation. These structured light illumination systems project a sinusoidal pattern onto specimens by placing a one-dimensional grating in the microscope's illumination path. This pattern is focused only at the in-focus plane of the specimen, where the image, I_1 is acquired. Movement of the grating by a third and two thirds of its cycle to positions where further images are acquired (I_2 and I_3 respectively) generates images in which only in-focus data is modulated by the grid pattern, while out-of-focus information is largely unaffected (i.e., constant in the three images). Subtraction of pairs of these images as described in the equation below removes both the grid pattern and the out-of-focus information and retains only in-focus information in the resultant image (Conchello and Lichtman, 2005; Neil et al., 1997).

$$\text{Confocal Image} = \sqrt{((I_1 - I_2)^2 + (I_1 - I_3)^2 + (I_2 - I_3)^2)}$$

Such structured light illumination systems effectively confer confocal capabilities to widefield microscopes. Although it is clear that the generated images are free from out-of-focus blur (Neil et al., 1997), their suitability for quantitative studies of fluorescently labeled specimens has not been demonstrated.

To determine whether a well-documented biological process could be quantitated, we chose the uptake and recycling of labeled transferrin. Transferrin and other plasma membrane receptor ligands are rapidly internalized after binding in clathrin-coated pits (Ullrich et al., 1996). The receptor is separated from the ligand in peripheral tubulovesicular sorting endosomes and is recycled to the plasma membrane through the endosomal processing pathway, the perinuclear recycling center and recycling endosomes. The process is mediated by several accessory proteins such as dynamin and TTP (Tasoni et al., 2005) and is independent from other plasma membrane receptor mediated endocytic pathways (Warren et al., 1997). The pathway is highly conserved in most eukaryotic cells.

To demonstrate the efficacy of using structured illumination and image processing to quantitate fluorescent images, we have undertaken studies of both a simple series of fluorescent standards and a more complex biological system—transferrin uptake and processing.

MATERIALS AND METHODS

Nonbiological Specimens

Fluorescence standards were prepared from an InSpeck Green (6 μm) microscope image intensity calibration kit (Molecular Probes, www.probes.com, cata-

*Correspondence to: Dr. Andrew Barlow, Improvision Ltd., Viscount Centre II, University of Warwick Science Park, Millburn Hill Road, Coventry, CV4 7HS, UK, 44-247-669-2229. E-mail: a.barlow@improvision.com

Received 7 April 2006; accepted in revised form 16 September 2006
DOI 10.1002/jemt.20389
Published online 27 November 2006 in Wiley InterScience (www.interscience.wiley.com).

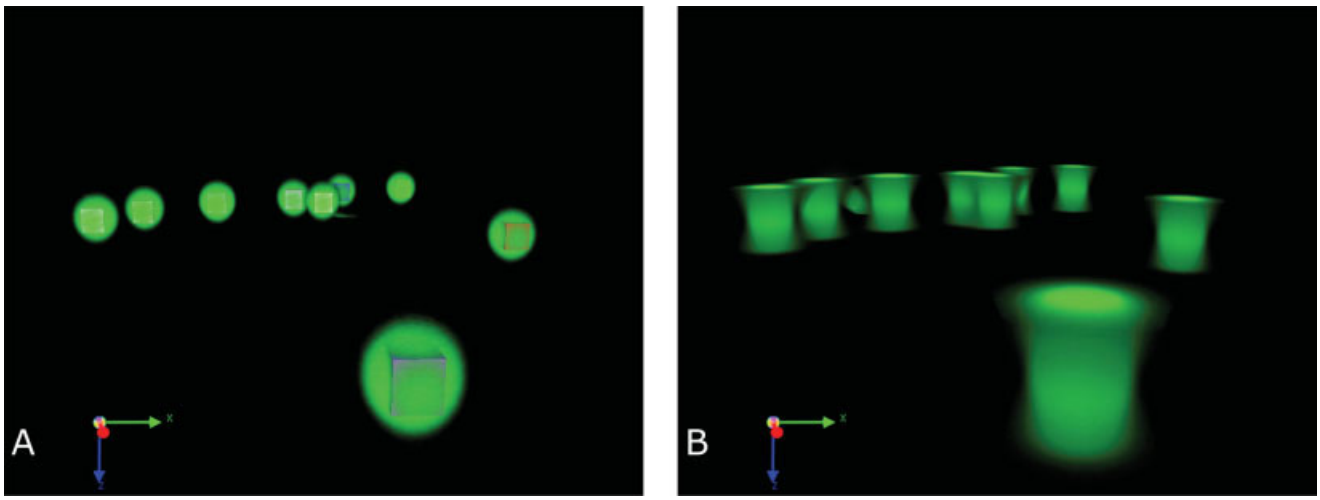

Fig. 1. **A**: 3D view of a field of 6 μm InSpeck beads acquired in Volocity grid confocal mode. The ROIs used to measure the intensity of the beads are shown within the beads. Note the spherical appearance of all the beads. **B**: 3D view of the same field of Inspeck beads as (A), acquired in grid widefield mode. Note that the true shape of the beads cannot be seen in this volume.

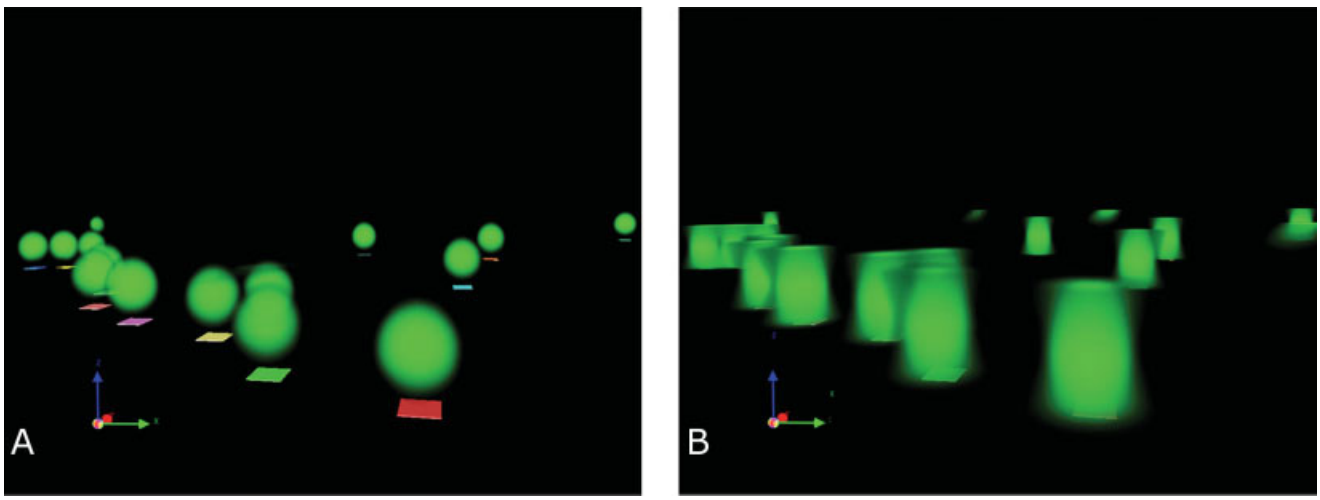

Fig. 2. **A**: 3D view of a field of 6 μm InSpeck beads acquired in Volocity grid confocal mode. The ROIs used to measure the intensity of a plane outside the beads are shown beneath the beads. **B**: 3D view of the same field of Inspeck beads as (A), acquired in grid widefield mode. The ROIs used to measure the intensity of a plane outside the beads are shown beneath the beads. [Color figure can be viewed in the online issue, which is available at www.interscience.wiley.com.]

logue Number I14785). Slides were prepared by drying 5 μL of components C, D, E, F, and G onto glass slides and by mounting in 10 μL of mounting medium (component H). This produced intensity standards of 1.2% relative intensity (RI), 3.4% RI, 11% RI, 33% RI, and 100% RI. All the beads were at the same depth (in contact with the slide).

Slides were imaged with a Zeiss Axiovert 200M microscope (www.zeiss.de) equipped with an Optigrid (Qioptiq, www.qioptiqimaging.com), a Zeiss number 10 filter block, an Orca ERG CCD camera with a cell size of 6.45 μm^2 (Hamamatsu Photonics, www.hamamatsu.com), and an Exfo 120 light source (Exfo, www.exfo-lifesciences.com). The microscope, camera, and Optigrid were controlled from an Apple G5 computer (Apple Computers, www.apple.com) running Volocity 3.6 (Improvision Ltd., www.improvision.com). All the images were acquired for this study using a 63 × plan apochromat (1.4 NA) oil immersion lens (Zeiss).

Exposure times were set by using the Volocity "auto-exposure" function with the 100% RI slide mounted. The same exposure time was used for all the other intensity standards; no microscope, light source, or camera controls were changed during the acquisition of an intensity standard series. The same exposure time was used for the acquisition of both grid confocal and grid widefield images; however, a different exposure time was used for the acquisition of true widefield images (removal of the Optigrid from the illumination system allows more light to reach the specimen). The camera gain and offset were both at their minimal settings.

Volumes 8 μm thick were acquired of the 6 μm thick beads, ensuring that the whole of the beads were imaged. The step size was 100 nm in depth. Each volume was composed of 81 *z*-sections.

A three-dimensional region of interest (ROI) containing 7,616 voxels (total volume 18.7 μm^3) was drawn entirely within a bead. The mean intensity within the ROI was measured. This was repeated for every bead within a single field of view for each RI sample and the mean of the mean intensities was calculated using the Volocity measurement functions. The same ROI was used for all measurements. When moving the ROI between beads, the position of the ROI was carefully checked in the *xy*, *xz*, and *yz* views to ensure that the entire ROI was entirely within the area of the bead (see Fig. 1).

The intensity of a single plane outside, but directly above the bead (plane 0, furthest from the light source), was also measured to determine how effectively fluorescence was contained within the bead for each of the imaging techniques. This ROI was exactly the same shape (in *x* and *y*) as the ROI used to measure the intensity within the bead and was drawn within a single plane directly above the ROI within the bead (see Fig. 2). This ROI contained 272 pixels (total area 6.7 μm^2). This method of measuring light intensity outside the bead was chosen in favor of other methods such as measurement of bead volume, as it is does not require an arbitrary intensity threshold in order to delimit bead and background.

The Hamamatsu Orca ERG camera has a built-in DC offset value of about 200 levels. This value is removed from OptiGrid confocal data by the algorithm used to generate the confocal images (in common with out-of-focus light, it is a constant between the three raw images) but is likely to adversely affect the accuracy of widefield data. We therefore removed 200 gray levels from all widefield mean intensities and 600 gray levels from all OptiGrid widefield mean intensities (OptiGrid widefield images are generated by adding the three images). The results of this bead intensity study were compared with and without this background correction.

In Vitro Studies

Cell Culture. HeLa cells were obtained as a frozen stock (Karolinska Institutet, Stockholm Sweden) and were cultured in DMEM with glutamate, 10% fetal bovine serum and penicillin/streptomycin (Invitrogen, http://www.invitrogen.com/). Cells were grown on 24 mm diameter round coverslips. Thirty minutes before the experiment was started, the media was changed to MEM without additives or phenol red (Invitrogen), and the coverslips were placed in a POC-R mini culture chamber (Zeiss). The chamber was mounted on a CO_2 and humidity controlled heating stage (temperature insert P, Incubator S, Zeiss) on an Axiovert 200M microscope with a plan-apochromat 63× (1.4 NA) oil immersion lens (Zeiss). The microscope was fitted with an Optigrid (Qioptic), an Exfo 120 light source, and a XS555/25 × excitation filter 62000v2bs triple dichroic and 61000v2m emission filter (Chroma, www.Chroma. com). All imaging was done with the Exfo light source set to 12% of maximum illumination. After thermal equilibrium was reached, recordings of *z* stacks were begun and taken at 2 min intervals. After the first three time points were collected, the medium was changed to MEM with

TABLE 1. The measured intensity of beads acquired with grid confocal, grid widefield, and true widefield imaging

Known relative intensity (%)	Grid confocal			Grid widefield			Widefield			Grid widefield corrected			Widefield corrected		
	Mean intensity (SD)	*n*	Measured relative intensity (%)	Mean intensity (SD)	*n*	Measured relative intensity (%)	Mean intensity (SD)	*n*	Measured relative intensity (%)	Mean intensity	*n*	Measured relative intensity (%)	Mean intensity	*n*	Measured relative intensity (%)
100	2177.0 (200.5)	15	**100**	4664.8 (414.4)	15	**100**	2887.9 (115.9)	4	**100**	4064.8	15	**100**	2687.9	4	**100**
33	686.7 (81.3)	12	**31.5**	1881.2 (113.7)	12	**40**	1003.2 (31.6)	5	**34.7**	1281.2	12	**31.5**	803.2	5	**29.9**
11	249.5 (17.1)	5	**11.4**	1000.6 (25.2)	5	**21**	470.4 (6.7)	9	**16.3**	400.6	5	**9.9**	270.4	9	**10.1**
3.4	82.7 (3.3)	11	**3.8**	732.1 (6.4)	11	**15.7**	284.2 (4.4)	9	**9.8**	132.1	11	**3.3**	84.2	9	**3.1**
1.2	29.5 (1.3)	9	**1.4**	634.7 (2)	9	**13.6**	226.8 (2.7)	9	**7.8**	34.7	9	**0.9**	26.8	9	**1**

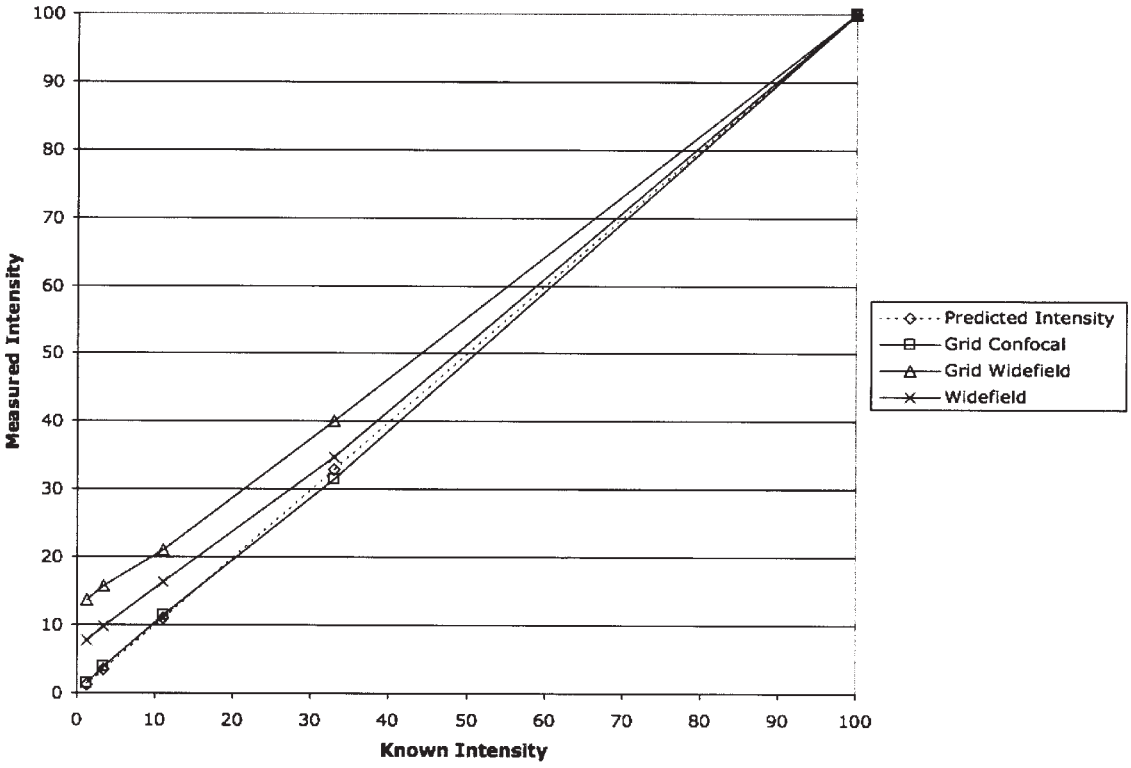

Fig. 3. Chart showing measured intensity versus predicted intensity of InSpeck beads with uncorrected data. Data were acquired in grid confocal mode, grid widefield mode, and widefield mode. Predicted intensities are also plotted.

10 μg/mL AlexaFluor 546 labeled transferrin (Invitrogen). The cells remained in this medium for 15 min, and then the medium was changed to MEM with 10% FCS (Sigma, www.sigma-aldrich.com). Recordings continued at 2 min intervals for another 10 min, and then the intervals between *z* stack recordings was lengthened to 6 min to minimize the effects of photo bleaching and toxicity.

Image Acquisition and Processing. Images were acquired with an Orca ERG camera with a cell size of 6.45 μm^2 (Hamamatsu) which was fitted to the side port of the microscope via a 0.63 × c-mount. The camera was set to a binning value of 2 × 2, the exposure was 250 ms, and the camera gain was set to the minimum value.

Volumes for each image stack were 5 μm thick, which imaged the full thickness of the cell. The step size was 0.5 μm in depth, which resulted in volumes composed of 11 *z*-sections. This relatively large *z* depth was selected in order to minimize bleaching artifacts over our time courses. We feel that under-sampling across the time course does not interfere fundamentally with the quantization, as it is constant across the whole time course and still allows us to observe relative changes between time points with accuracy. All measurements were performed using Volocity 3.6.1 (Improvision). Noise was removed from all image sequences using a 3 × 3 median filter. The mean background intensity (from an area in which no cells were present) was calculated for each time series. A classifier was made to measure all objects that were greater than 4 × brighter than the background; the classifier excluded any objects with a volume smaller than 0.25 μm^3 (5 voxels). In the case of the fixed control cells, which had a much lower background than the experimental cells (all labeled medium was thoroughly washed away), the 4 × background rule was not applied. Instead, a classifier was made by adjusting the intensity threshold of the classifier until the number of objects selected at the start of the time course was similar to the number selected in the live cell experiments at the start of the time course.

Measurements tables were exported from Volocity to Excel (Microsoft, www.microscoft.com) for further analysis. The total volume of all the objects recorded for each time point was calculated, and the charts showing the total volume per time point were plotted.

RESULTS

Nonbiological Specimens

The mean intensity of beads acquired with grid confocal, grid widefield, and true widefield imaging are shown in Table 1 and are plotted in Figure 3. Figure 3 shows that of the three techniques used to acquire the data, grid confocal shows relative intensities closest to the predicted values without any further manipulation of data. Following correction of data by removing the known camera DC offset value of 200 from widefield images and 600 from grid widefield images, the measured intensities from all techniques closely match the predicted intensities (see Table 1 and Fig. 4).

When the mean intensity of a plane outside the beads was measured, the grid confocal images proved

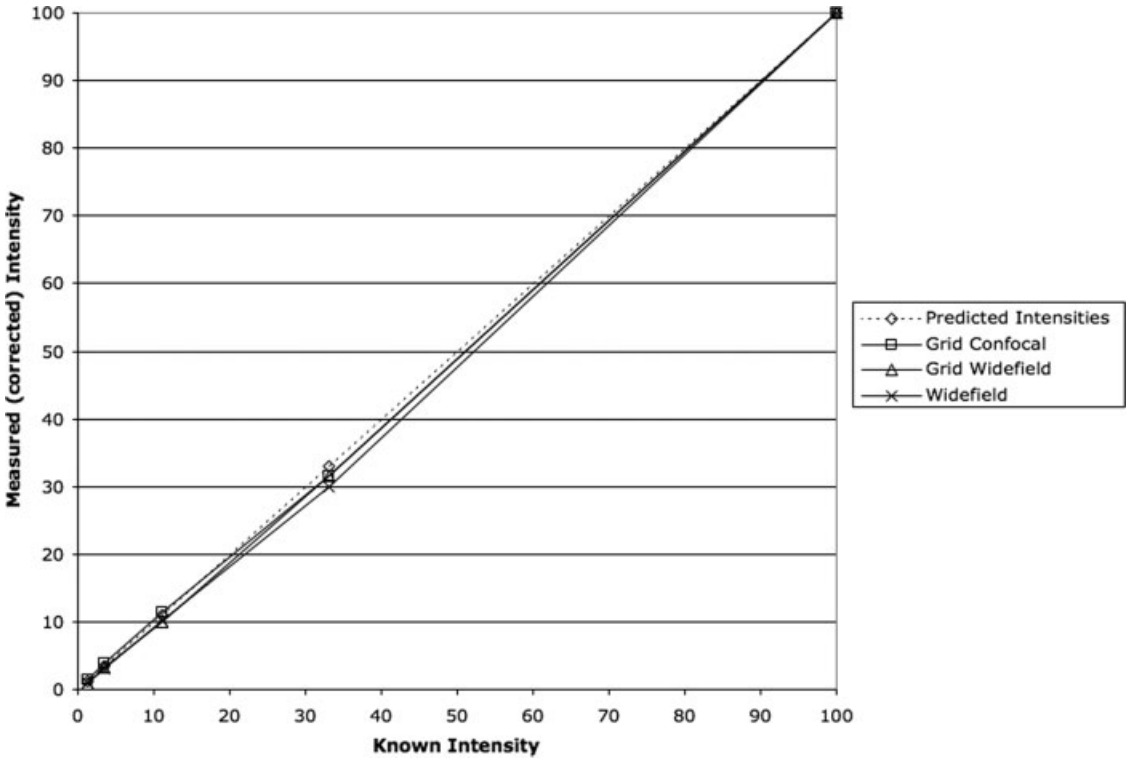

Fig. 4. Chart showing measured intensity versus predicted intensity of InSpeck beads with background corrected data. Data were acquired in grid confocal mode, grid widefield mode, and widefield mode. Predicted intensities are also plotted.

TABLE 2. The mean measured intensity of a plane outside the beads acquired with grid confocal, grid widefield, and widefield imaging

Relative intensity (%)	Mean measured intensity (gray level)					
	Grid confocal		Grid widefield (corrected)		Widefield (corrected)	
	Inside	Outside (% of inside)	Inside	Outside (% of inside)	Inside	Outside (% of inside)
100	2177.0	85.3 (3.9)	4064.8	1879.5 (46.2)	2687.9	1355.3 (50.4)
33	686.7	73.9 (10.7)	1281.2	881.8 (68.8)	803.2	352.1 (43.8)
11	249.5	30.1 (12.1)	400.6	207.3 (51.7)	270.4	169.5 (62.7)
3.4	82.7	22.4 (27.1)	132.1	84.4 (63.9)	84.2	45.2 (53.7)
1.2	29.5	16 (54)	56.4	20.2 (35.8)	26.8	9.9 (36)

far more effective than the other techniques at isolating bright fluorescence within the bead than either grid widefield or widefield images, particularly with high relative intensities (see Table 2 and Figs. 5 and 6).

In Vitro Studies

We were able to effectively generate 3D volumes of transferrin labeled cells that contained greatly reduced amounts of out-of-focus information using our structured light illumination system (compare Figs. 7A and 7B). We were able to generate these images over periods of several hours (up to 12, see time course 3 in Fig. 8). Transferrin was initially found in the cell periphery in sorting endosomes (Fig. 9A), with the endosomes moving to the perinuclear recycling center with increasing time (Figs. 9B and 9C). Intensity of the endosomes decreased towards the end of the time course (see Fig. 9D) before being entirely lost through dilution with unlabeled transferrin by the end of the time course. The total volume of transferrin detected over time for three separate experiments is shown in Figure 8. After a period, during which the volume of labeled transferrin remained relatively stable (time points 20–40 in time course 1, time points 20–30 in time course 2), we saw a rapid decline in the volume of labeled transferrin in time courses 1 and 2. Time course 3 differed somewhat from time courses 1 and 2 in that we saw a much more gradual decline in the volume of labeled transferrin present in the cells, which took place over an extended period (12 h).

DISCUSSION

The results presented demonstrate that it is possible to precisely quantitate images produced from a widefield microscope. The use of a structured illumination system which eliminates out-of-focus light, thus reducing background noise, allows for accurate identification of fluorescent signal free of artifactual content. In the

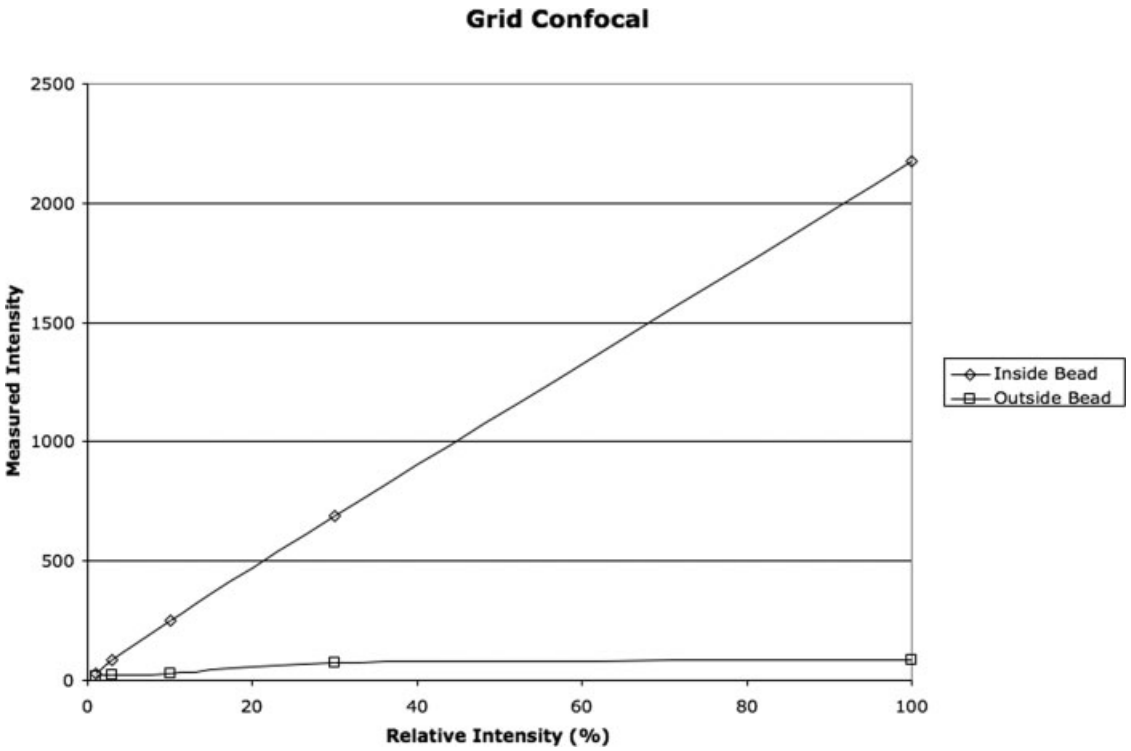

Fig. 5. Chart showing the measured intensity (gray levels) for a 3D ROI within the 6 μm InSpeck beads (inside bead, diamonds), and a 2D ROI beneath the beads (outside bead, squares) for data acquired in grid confocal mode. No further corrections were made to the data.

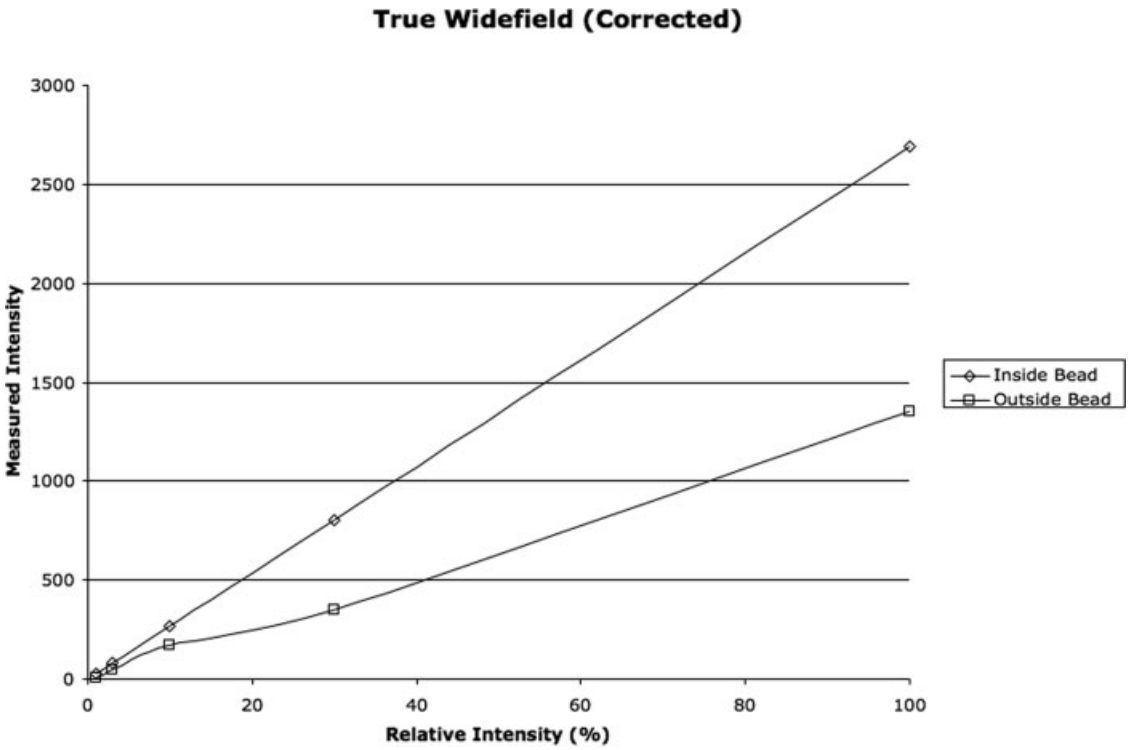

Fig. 6. Chart showing the measured intensity (gray levels) for a 3D ROI within the 6 μm InSpeck beads (inside bead, diamonds), and a 2D ROI beneath the beads (outside bead, squares) for data acquired in widefield mode. The data were background corrected by subtracting 200 gray levels from the data.

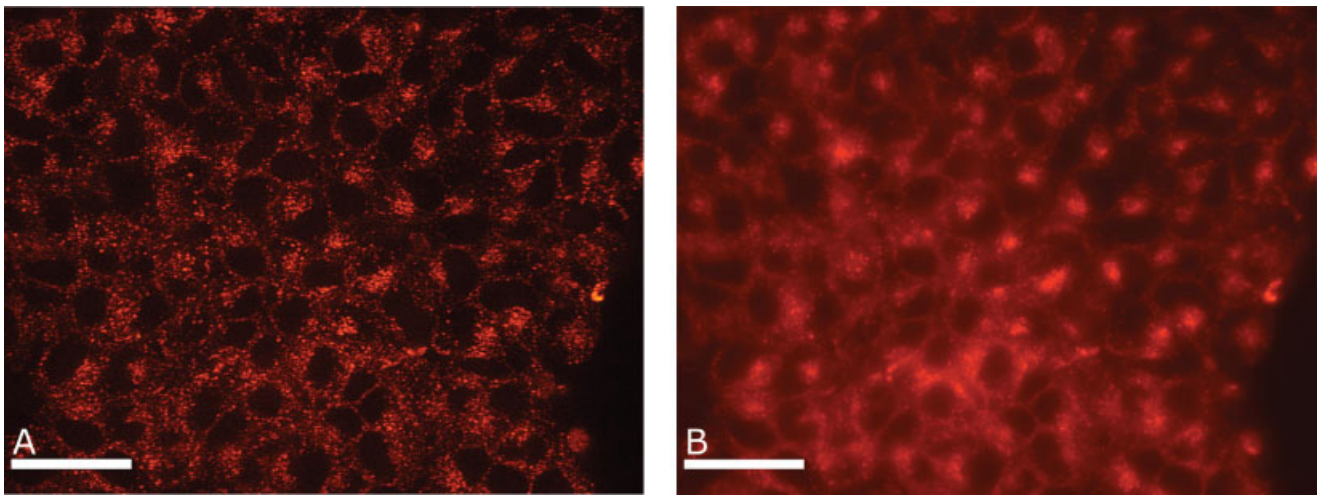

Fig. 7. **A**: Maximum intensity projection of a field of HeLa cells after incubation with labeled transferrin in grid confocal mode. Scale bar = 40 μm. **B**: Maximum intensity projection of the same field of HeLa cells as (A), in this case in grid widefield mode. Scale bar = 40 μm. The increase of detail when using the grid system is apparent.

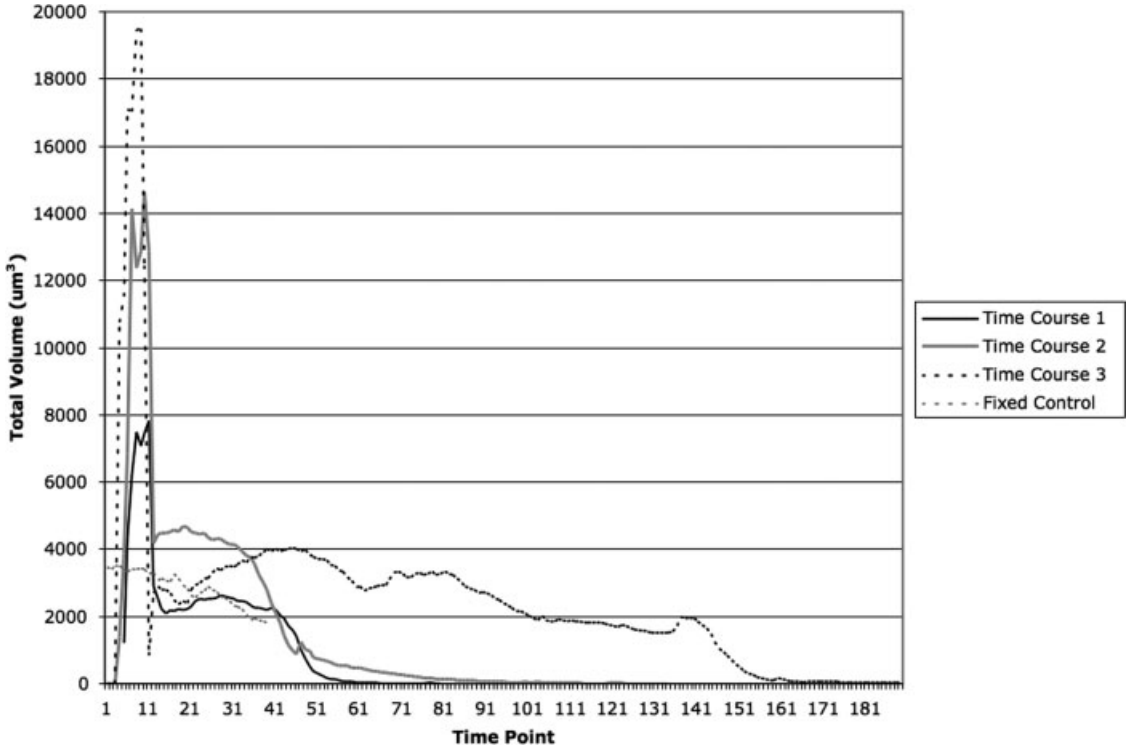

Fig. 8. Chart showing the total volume of labeled transferrin measured versus time. Time courses 1–3 were measured in live HeLa cells, and the control was measured in fixed HeLa cells.

bead sample, the grid confocal system produced values much closer to the known relative intensities than the uncorrected widefield or uncorrected grid widefield systems (Fig. 3), especially in the samples with faint signals. After background correction of widefield and grid widefield images, the RI measured with these techniques also closely resemble the predicted values. These results illustrate some important findings regarding grid confocal images. First, the processing of raw data through the algorithm of Neil et al. (1997) to generate confocal images preserves the RI of specimens. Second, background subtraction becomes unnecessary with grid confocal images, removing a processing step without which widefield and grid widefield images become increasingly inaccurate, as relative intensities decrease (see Table 1).

Perhaps more importantly, bright fluorescence signals are much more effectively confined within the

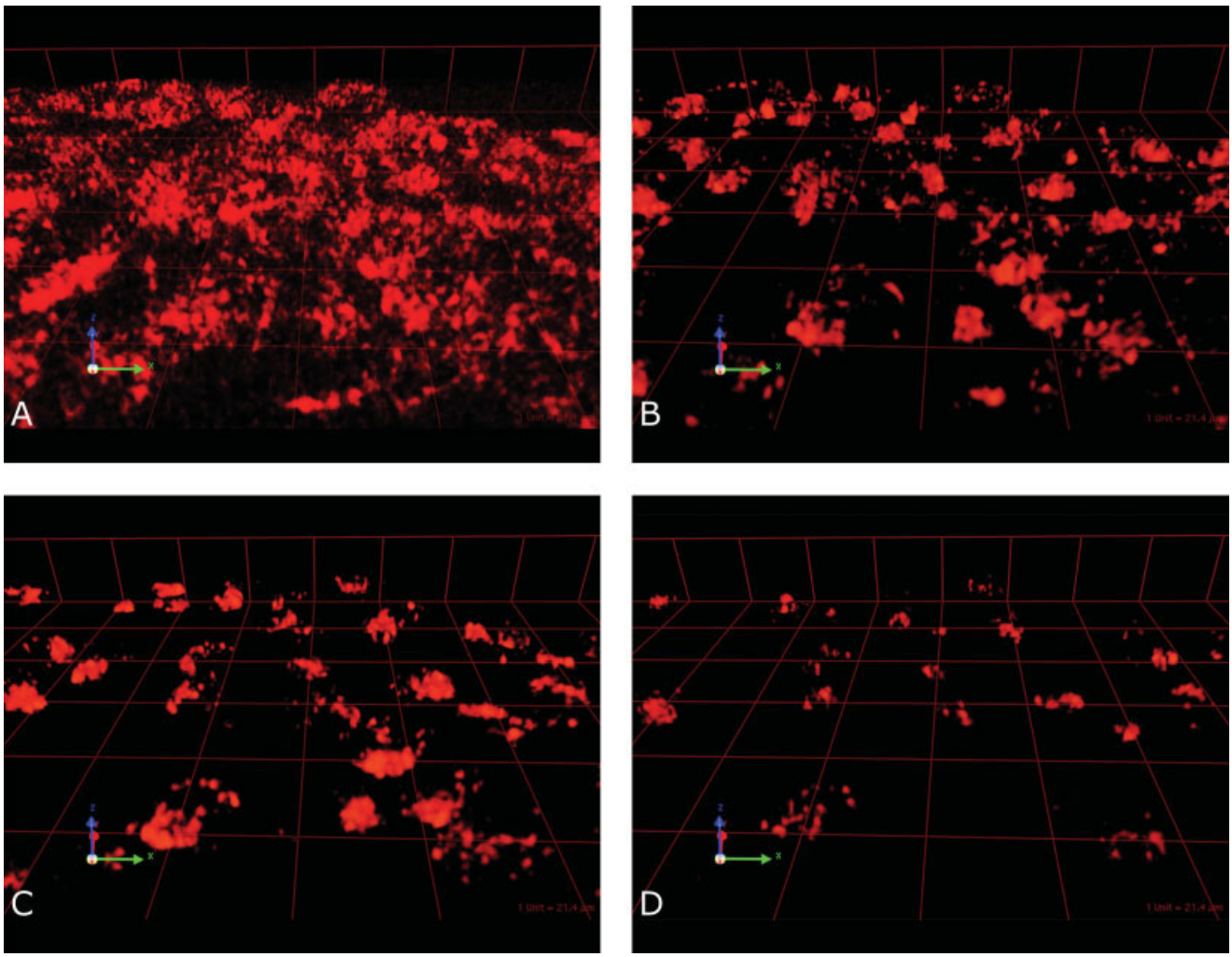

Fig. 9. 3D rendering of HeLa cells after 6 (**A**), 14 (**B**), 37 (**C**), and 54 (**D**) time points. Note the changing distribution of labeled transferrin throughout the time course. Transferrin is initially seen in peripheral sorting endosomes (A), which move to the perinuclear recycling center (B and C). The intensity of the endosomes decreases towards the end of the time course. 1 scale unit = 21.4 μm. [Color figure can be viewed in the online issue, which is available at www.interscience.wiley.com.]

beads with grid confocal images than with widefield images (see Table 2 and Figs. 5 and 6). Although reasonably accurate measurements can be made in widefield systems, the accuracy of these measurements is dependant upon there not being other bright fluorescent structures in planes above or below objects of interest. This is the limitation that effectively makes it impossible to guarantee that intensity measurements made in widefield systems are measurements of light originating within the object of interest. The ability of grid confocal imaging to confine fluorescence to the objects in which it originates, combined with our observation that intensity measurements made with the grid confocal system preserves the RI of specimens, makes it a much more credible system for performing quantitative fluorescence measurements.

Quantitating fluorescent images requires preparations where the signal to noise ratio (SNR) is high. To achieve this some method for eliminating out-of-focus information is necessary. Image manipulation such as the application of filters can reduce background noise; however, the possibility exists that some of the true signal might be lost in the process. One solution is to use variable pinholes such as are found in laser scanning confocal microscope systems (White et al., 1987) or a spinning disk which creates a virtual pinhole by removing oblique illumination (Nakano, 2002). While both of these solutions produce excellent results, they do require a significant financial investment in acquiring the technology.

Another factor which can degrade the data produced from fluorescent information is photobleaching. Using a fixed specimen, we measured the effects of repeated illumination using the same parameters as in our living preparations. Even with minimizing the light intensity and time of exposure, a portion of the signal was lost to photobleaching. This complication is particularly critical when background noise is high, since the signal is degraded more intensely than the background reducing the SNR. In our experiments, we were able to accurately measure transferrin internalization and

degradation over prolonged periods of time despite the loss of signal which was due to photobleaching.

The distribution of transferrin which we observed during our time courses fitted with that observed by others (Ullrich et al., 1996). We observed very high volumes during the period when the labeled transferrin was free in the medium (time points 3–10), which was greatly reduced after switching to label free medium. These peaks observed are largely due to the presence of free label in the medium, which generates general fluorescence that was measured by the image analysis classifier. The levels of labeled transferrin after removal of the labeled medium at time point 10 gives a much more accurate measurement of bound transferrin. Following removal of labeled transferrin from the medium, the volume of transferrin continued to increase reflecting the lag time between when transferrin is bound in clathrin coated pits and its transfer to sorting endosomes. Only when the accumulation of transferrin exceeds a minimum resolvable level, (0.25 μm^3 under the optical conditions used in this experiment), is it counted by the image analysis algorithm. The time course of degradation for the first two experiments was shorter than for experiment 3. The variation could be due to the larger initial loading and/or to temperature variation which can occur despite the use of a heated stage.

The use of structured illumination has demonstrated that simple intensity measurements can be very accurately determined in a widefield system. This is a critical factor in obtaining accurate signals which are necessary when using fluorescently tagged compounds in biological experiments. The results of the transferrin experiments demonstrate that such clear information, when combined with computer assisted image analysis, allows the morphological information to be accurately quantified. Combining these two components, biological phenomena such as the volumes of subcellular structures can be measured and their dynamics studied in living specimens.

ACKNOWLEDGMENTS

We are grateful to Dr. Edward Bampton, Dr. David Dinsdale, Dr. Paul Richards, Steve Baxter and Claire Stewart for helpful comments on the manuscript. We would also like to thank Andrew Waterfall for providing transferrin and for the loan of the Optigrid structured light system.

REFERENCES

Conchello JA, Lichtman JW. 2005. Optical sectioning microscopy. Nat Methods 2:920–931.

Nakano A. 2002. Spinning-disk confocal microscopy—A cutting-edge tool for imaging of membrane traffic. Cell 27:349–355.

Neil MAA, Juskaitis R, Wilson T. 1997. Method of obtaining optical sectioning by using structured light in a conventional microscope. Opt Lett 22:1905–1907.

Tosoni D, Puri C, Confalonieri S, Salcini AE, De Camilli P, Tacchetti C, Di Fiore PP. 2005. TTP specifically regulates the internalization of the transferrin receptor. Cell 123:875–888.

Ullrich O, Reinsch S, Urbé S, Zerial M, Parton RG. 1996. Rab 11 regulates recycling through the pericentriolar recycling endosome. J Cell Biol 135:913–924.

Warren RA, Green FA, Enns CA. 1997. Saturation of the endocytic pathway for the transferrin receptor does not affect the endocytosis of the epidermal growth factor receptor. J Biol Chem 272:2116–2121.

White JG, Amos WB, Fordham M. 1987. An evaluation of confocal versus conventional imaging of biological structures by fluorescence light microscopy. J Cell Biol 105:41–48.

Yuste R. 2005. Fluorescence microscopy today. Nat Methods 2:902–904.